

## Ultrasound-Induced Nucleation in Microcellular Polymers

Abhishek Gandhi, Neelanchali Asija, Hemant Chauhan, Naresh Bhatnagar

Department of Mechanical Engineering, Indian Institute of Technology, Delhi Hauz Khas, New Delhi, 110016, India

Correspondence to: N. Bhatnagar (E-mail: narbhat@hotmail.com or nareshb@mech.iitd.ac.in)

**ABSTRACT:** In this study, microcellular Acrylonitrile–Butadiene–Styrene foams with high cell density and expansion ratio has been manufactured using ultrasound-induced nucleation technique in solid-state batch foaming process. Influence of sonication time, sonication frequency, and ultrasound power were found very crucial in designing of cellular morphology. The initial 10 s of ultrasound exposure was found to influence the foam morphology critically. Longer periods of ultrasound exposure developed foams with lower average cell size as compared to foams developed with lesser ultrasound exposure time. Higher sonication power resulted in foams with uniform morphology and higher cell densities as compared to foams developed with lower sonication intensities. Finally, the ultrasonic frequency was also found to influence the morphology intensely. Low frequency sonication resulted in foams with uniform cell distribution, whereas high frequency sonication developed bimodal microcellular type of microstructure. The results coherently demonstrate that with the advent of ultrasonic waves, the energy barrier for cell nucleation swiftly decreases which enhances the cell density in the final foamed product. © 2014 Wiley Periodicals, Inc. *J. Appl. Polym. Sci.* **2014**, *131*, 40742.

**KEYWORDS:** manufacturing; microscopy; morphology; porous materials; thermoplastics

Received 13 December 2013; accepted 20 March 2014

DOI: 10.1002/app.40742

### INTRODUCTION

Microcellular microstructure in polymers offers numerous benefits such as reduced material with superior mechanical properties,<sup>1–3</sup> in comparison to their unfoamed counterparts. They have a tremendous potential applications prospect in fields of automobiles, packaging, aerospace, and biomedical.<sup>4–8</sup> Over the past few decades, considerable efforts has been put through to achieve such a structure in various polymeric systems,<sup>9–12</sup> yet scientists continue to find newer techniques to develop microcellular microstructure foams having higher expansion ratio along with high cell densities.<sup>13–15</sup>

Solid-state microcellular batch foaming requires a very high nucleation as compared to the conventional macroscaled foams. Addition of nanosized fillers has been found to considerably increase the cell density by reducing the energy barrier or nucleation, yet the stiffness of this nanocomposite became a limiting factor in achieving high expansion ratio.<sup>16</sup> Another strategy utilized by scientists is to increase the physical blowing agent content. Owing to low solubility of gases in polymers, setups involving high gas pressures were developed which incurred huge costs and were not easy for the industry to accept. More recently scientists utilized ultrasonic waves as a promising solution to this problem.<sup>17,18</sup>

Ultrasound produces a huge number of cavitation bubbles inside a liquid medium, which on collapsing develops local

extreme conditions of high temperature and high pressure. As the ultrasonic pressure wave propagates, it develops negative pressure, which significantly improves the cell nucleation phenomenon.<sup>19,20</sup> This technique was successfully utilized in polystyrene<sup>17</sup> and Polylactic acid<sup>18</sup> systems to enhance both cell densities and expansion ratios.

In this article, ultrasound-induced nucleation technique has been utilized on acrylonitrile–butadiene–styrene (ABS) polymeric system to design the cellular morphology. Significant effects of sonication on foaming process have been investigated, which could certainly enhance the understanding of scientists and researchers on this broad emerging interdisciplinary field.

### EXPERIMENTAL

#### Material

ABS (Lustran ABS M-204) was used as the base polymer for this study. Physical blowing agent used was CO<sub>2</sub> gas supplied at a pressure of 6 MPa.

#### Foaming Methodology

Injection molded specimens of 1.5-mm thickness were placed in a vessel under high pressure CO<sub>2</sub> gas for a specific amount of time. After saturation, the samples were placed in water bath at 60°C, having ultrasonic transducer systems (Martin-Walter push-pull transducer 25 and 45 KHz), for a certain amount of time and then were dipped inside hot glycerin bath at a

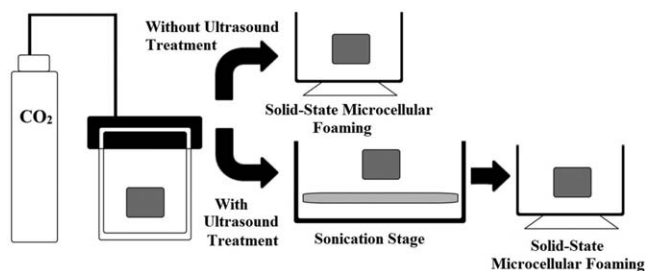


Figure 1. Experimental setup.

temperature termed as foaming temperature. Foaming time was selected to be approximately 20 s for all the cases, after which these were quenched in water at room temperature (Figure 1). Gas sorption study was performed at various saturation pressures for a maximum time of 48 h. The gas uptake was calculated using gravimetric method as described in previous studies.<sup>2</sup>

### Foam Characterizations

The foamed samples were collected and placed inside liquid nitrogen for at least 10 min, after which they were fractured. The fractured surface was then analyzed for morphological attributes under the scanning electron microscope (Hitachi TM-1000). The average cell size was found by taking the average of

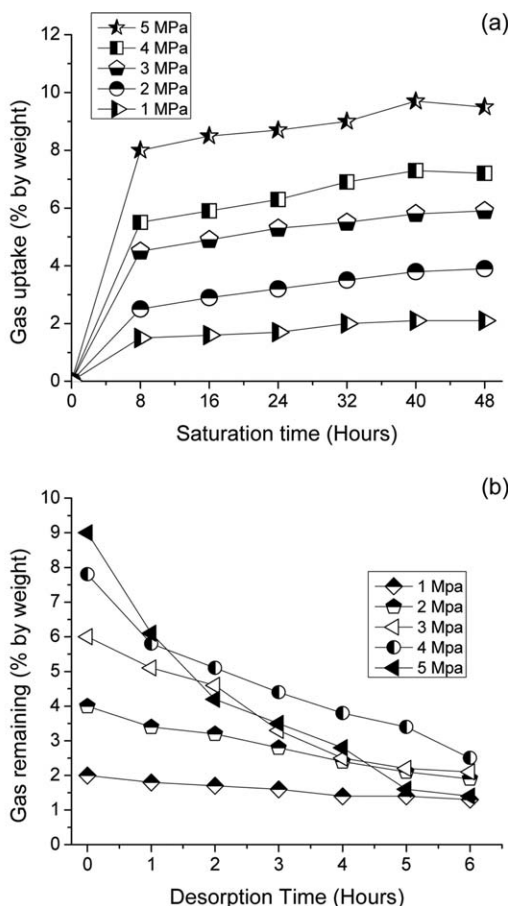


Figure 2. Sorption-Desorption curve for Acrylonitrile-Butadiene-Styrene at various saturation pressures. (a) Sorption curve and (b) Desorption curve.

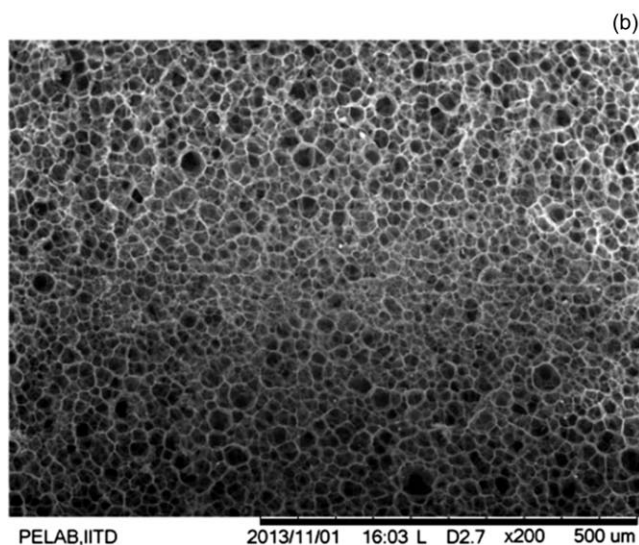
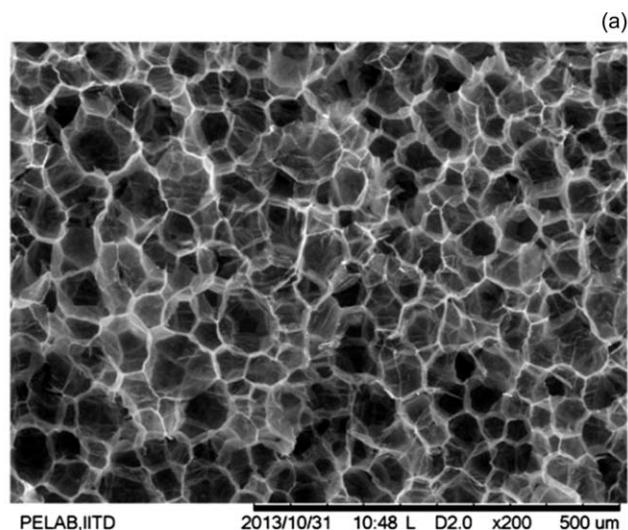


Figure 3. Sonication-induced nucleation: (a) without ultrasound exposure and (b) with ultrasound exposure.

100 cells from a particular SEM micrograph. Further, cell density ( $N_o$ ), the number of cells per cubic centimeter of solid polymer, was determined using eq. (1) as under

$$N_o = \left[ \frac{nM^2}{A} \right]^{3/2} \Delta \quad (1)$$

where  $n$  is the number of cells in the SEM micrograph, " $M$ " is the magnification factor, " $A$ " is the area of micrograph, and  $\Delta$  is the expansion ratio, which can be calculated by using eq. (2), as under

$$\Delta = \frac{\rho}{\rho_f} \quad (2)$$

where  $\rho$  and  $\rho_f$  are the densities of the unfoamed and foamed material, respectively.

## RESULTS AND DISCUSSION

### Sorption-Desorption Behavior of ABS

Gas saturation conditions play a very crucial role in microcellular foaming process. In general, high saturation time as well as

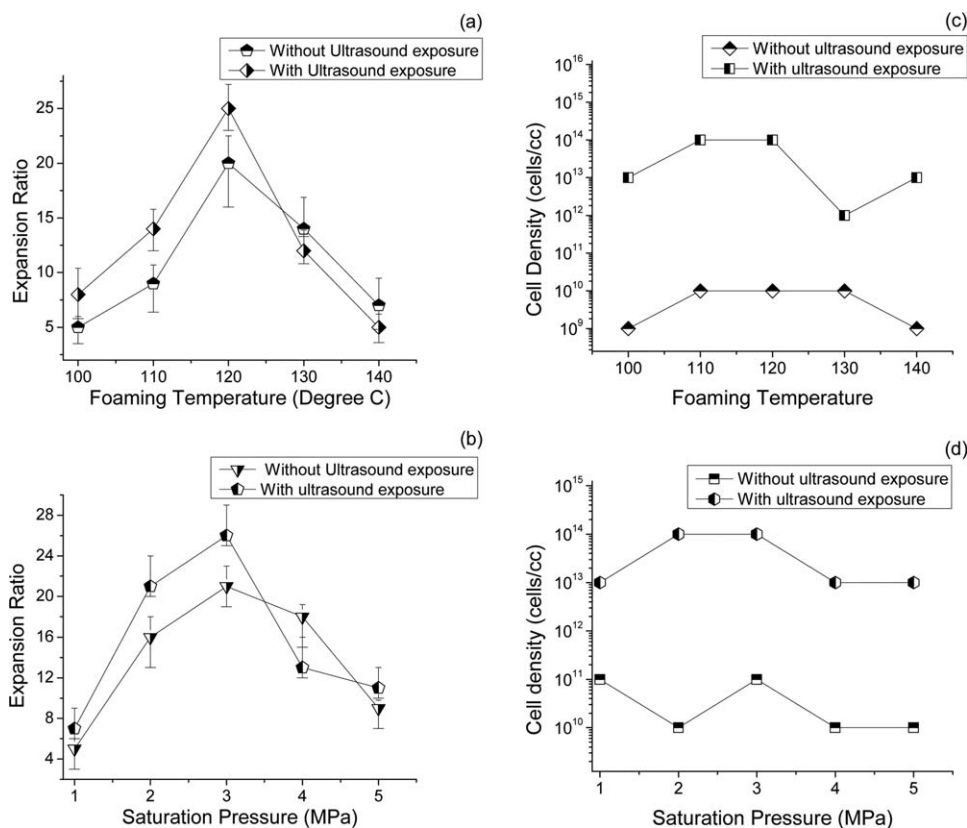


Figure 4. Effect of ultrasound waves on foaming at various foaming conditions.

high saturation pressure induces crystallization in the polymeric matrix, because of enhanced chain mobility. This induced crystallinity further effect the foam morphology.

Figure 2(a) shows the gas sorption curve for ABS-CO<sub>2</sub> system at various saturation pressures. Over time, the CO<sub>2</sub> concentration increases within the polymer until the polymer can no longer absorb any more gas, which is termed as the saturated state. The concentration of gas in ABS polymer increases as the saturation gas pressure is increased. At a saturation pressure of 1, 2, 3, 4, and 5 MPa, the maximum percentage of gas absorbed (by weight) were 1.9%, 2.6%, 5.1%, 5.9%, and 8.1%, respectively. Further experiments were performed with ABS saturated at 3 MPa CO<sub>2</sub> gas pressure (5.9% gas by weight).

Figure 2(b) shows the desorption curves at 27°C (room temperature), where the amount of gas was plotted as a function of time. It was observed that the samples saturated at high gas pressure desorbed at a much faster rate and gradient as compared to the samples saturated at lower pressures. Almost all the samples reached 2% gas content after a period of 6 h. This time period is significant in determining the maximum amount of time before which the polymer/gas system has to be processed.

### Influence of Ultrasonic Excitations on Microcellular Nucleation

The saturated samples at 3 MPa CO<sub>2</sub> gas pressure were transferred into a water bath at 60°C containing ultrasonic transducer system for a period of 10 s and then were placed inside hot glycerine. Figure 3 shows the SEM images of ABS

microcellular foams developed with and without ultrasound exposure. The average cell size without ultrasound exposure was found to be approximately 38 μm which significantly reduced to approximately 8 μm with ultrasound exposure as shown in Figure 3(a,b), respectively. The cell density was also found to considerably increase by the use of ultrasonic excitations before thermal instability.

To better understand the effect of such ultrasound excitations, a complete analysis was done, first by varying foaming temperature and then by varying saturating pressure. Investigation was done on saturation pressures ranging in between 1 and 5 MPa and foaming temperature between 100 and 140°C, as shown in Figure 4.

Foam expansion ratio increased as the foaming temperature was increased from 100 to 120°C [Figure 4(a)] due to softening of the polymer matrix, but as the temperature was further increased from 120 to 140°C, huge gas loss was observed due to which lower expansion ratio was achieved. With the use of ultrasonic excitations, expansion ratio of 25.8 was achieved at foaming temperature of 120°C. Further the cell density was also found to increase by an order of three with the sonic exposure [Figure 4(b)]. The reason behind this significant morphological upgradation is still not fully understood; although some works<sup>17–20</sup> suggest the cause could be the induction of high thermodynamic instability on the polymer/gas system.

The cell morphology in microcellular foaming occurs in three major stages, namely, cell nucleation, cell growth, and cell stabilization. The nucleation stage is directly controlled by the



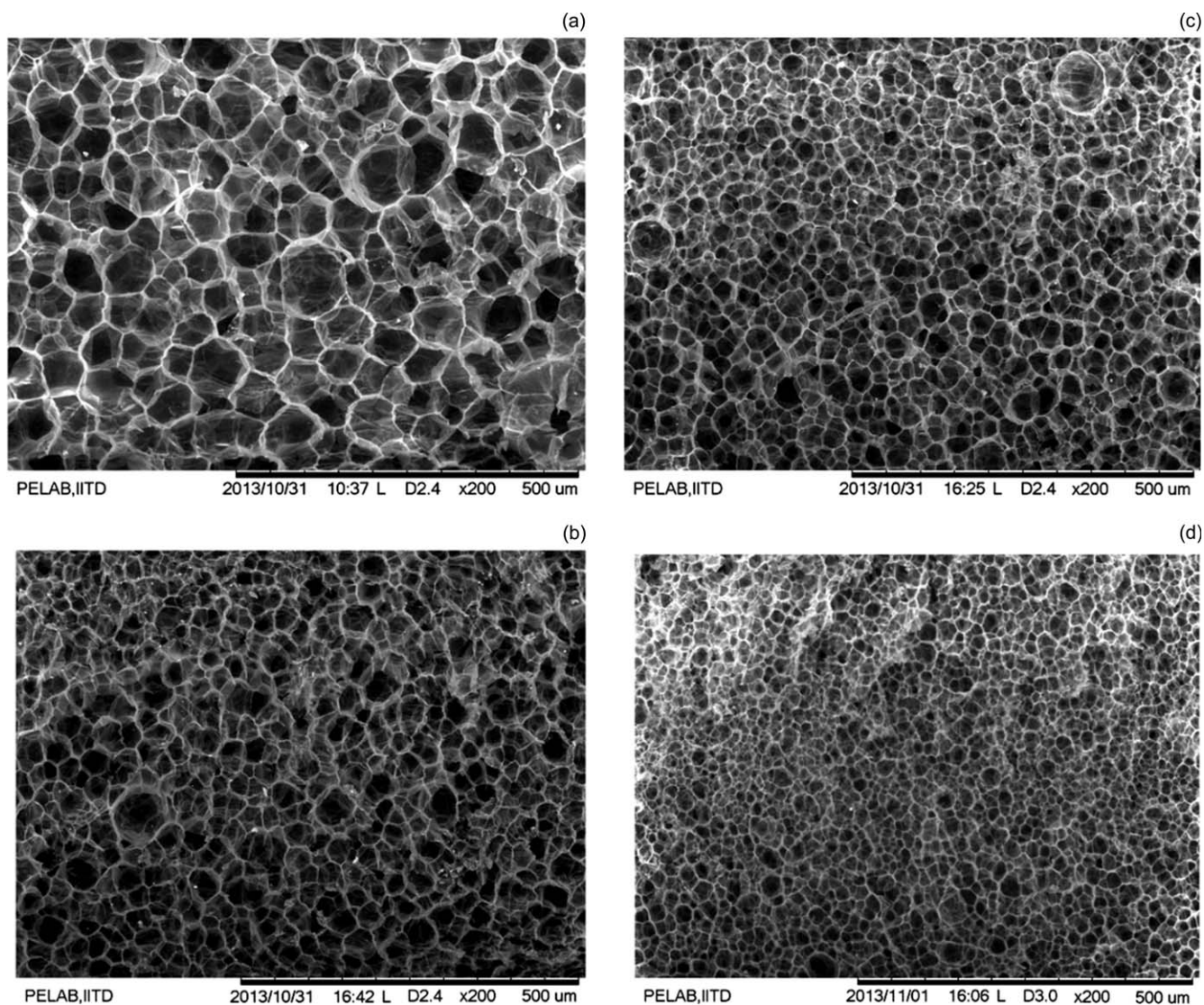


**Figure 5.** Influence of duration of ultrasound exposure on cell morphology: (a) 2 s, (b) 5 s, (c) 7 s, and (d) 10 s.

thermodynamic instability that is being induced on the polymer/gas system. Either a high pressure drop or a high temperature increment induces a high thermodynamic instability, which might be sufficient enough to nucleate microcellular cells.

In the case with ultrasound treatment, a large number of cavitation bubbles are developed which increases in their size over time. Once it reaches the critical size, it collapses violently and microjets are developed. These microjets bombard at the surface of the polymer with extremely high velocity creating high temperature and pressure at that localized area. This highly localized area is termed as hot spot which experiences extreme conditions of 5000°C and 1000 atm. These extreme conditions induce significantly high thermodynamic instability in polymer/gas system which eventually leads to high cell nucleation.<sup>17,18</sup>

Experiments performed on various saturation pressures revealed an optimum condition for achieving maximum expansion ratio. As the saturation pressure increased, the expansion ratio as well as cell density got increased, but after 3 MPa, cell densities

continued to elevate but expansion ratio reduced [Figure 4(c,d)]. Gas loss phenomenon was the main reason for this reduction in expansion ratio. With the introduction of ultrasound, a maximum expansion ratio of 25.8 was obtained at 3-MPa saturation pressure at 120°C foaming temperature. Conclusively, higher expansion ratios and cell densities were obtained with the utilization of ultrasonic waves.

#### Effect of Ultrasonic Parameters on Microcellular Foam Morphology

Figure 5 describes the influence of ultrasound exposure time on the morphology of the final foam product. It was observed that as the time increased, the morphology got more uniform along with reduced cell size and increased cell density. Also, maximum influence was observed at a time period of 10 s.

Figure 6 describes influence of ultrasonic frequency on the foam morphology. With 25-KHz frequency, uniform cell distribution was obtained, whereas with 45-KHz frequency bimodal type of morphology is observed. Although the average cell size decreased

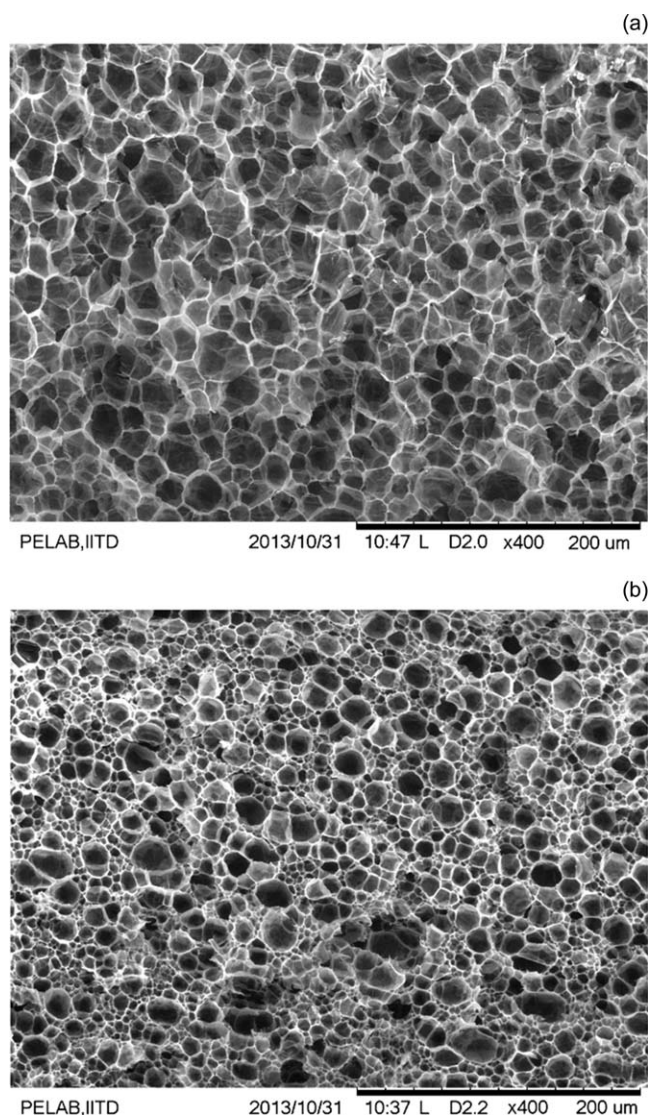


**Figure 6.** Influence of ultrasound frequency on foam microstructure. (a) Foam developed with 25-KHz frequency and (b) foam developed with 45 KHz.

by increasing the ultrasound frequency, yet the uniformity was disturbed and small bubbles were found to nucleate around bigger bubbles. The prime reason behind this phenomenon is yet unexplored, but the authors suggest that as with higher ultrasound frequency, the number of cavitation events increases, it leads to higher number of smaller hot spots. This develops a very large number of small cells. But as the microjets continue to impinge on the material, new cells nucleate around these growing cells, eventually leading to bimodal microcellular morphology foams, which can also be corroborated by the works of Arora et al.<sup>21</sup> and Baldwin et al.<sup>22</sup>

## CONCLUSIONS

In this article, influence of ultrasound excitations was found to significantly influence the foaming behavior of microcellular ABS foams. By increasing the ultrasound exposure time, cell

density increased tremendously. Also with sonication frequency 45 KHz, a special morphology of bimodal microcellular morphology was observed. Ultrasound exposure was found to induce a high thermodynamic instability in polymer/gas system which enhanced the cell density and decreased cell size. Cavitation bubble collapse leading to the development of microjets and hot spots were found responsible to develop such extreme conditions. This article intends to open a new interdisciplinary field of microcellular nucleation enhancement using ultrasound waves, which can be further utilized in numerous polymer systems to develop microcellular foams effectively and efficiently.

## REFERENCES

- Mi, H. Y.; Jing, X.; Salick, M. R.; Crone, W. C.; Peng, X. F.; Turng, L. S. *Adv. Polym. Technol.* **2014**, *33*, 1.
- Ma, Z.; Zhang, G.; Yang, Q.; Shi, X.; Shi, A. *J. Cell. Plast.* **2013**, *50*, 55.
- Gandhi, A.; Asija, N.; Gaur, K. K.; Rizvi, S. A. J.; Tiwari, V.; Bhatnagar, N. *Mater. Lett.* **2013**, *94*, 76.
- Yang, J.; Huang, L.; Zhang, Y.; Chen, F.; Zhong, M. *J. Appl. Polym. Sci.* **2013**, *130*, 4308.
- Li, J.; Chen, Z.; Wang, X.; Liu, T.; Zhou, Y.; Luo, S. *J. Appl. Polym. Sci.* **2013**, *130*, 4171.
- Gong, W.; Gao, J.; Jiang, M.; He, L.; Yu, J.; Zhu, J. *J. Appl. Polym. Sci.* **2011**, *122*, 2907.
- Miller, D.; Kumar, V. *J. Appl. Polym. Sci.* **2013**, *127*, 1967.
- Guo, H.; Nadella, K.; Kumar, V. *J. Mater. Sci.* **2013**, *28*, 2374.
- Guriya, K. C.; Tripathy, D. K. *J. Appl. Polym. Sci.* **1996**, *62*, 117.
- Deng, L. H.; Chen, Z. L.; Wang, F. *Adv. Mater. Res.* **2013**, *785*, 1041.
- Scattina, A. *Lat. Am. J. Solids Struct.* **2013**, *11*, 200.
- Han, E.; Cha, S. W. *Polym. Plast. Technol. Eng.* **2013**, *52*, 1290.
- Babaei, I.; Madanipour, M.; Farsi, M.; Farajpoor, A. *Compos. Part B* **2014**, *56*, 163.
- Ding, J.; Ma, W.; Song, F.; Zhong, Q. *J. Mater. Sci.* **2013**, *48*, 2504.
- Hwang, S. S.; Hsu, P. P. *J. Ind. Eng. Chem.* **2013**, *19*, 1377.
- Zhao, H.; Cui, Z.; Wang, X.; Turng, L. S.; Peng, X. *Compos. Part B* **2013**, *51*, 79.
- Zhai, W.; Yu, J.; He, J. *Polymer* **2008**, *49*, 2430.
- Wang, J.; Zhai, W.; Ling, J.; Shen, B.; Zheng, W.; Park, C.B. *Ind. Eng. Chem. Res.* **2011**, *50*, 13840.
- Byon, S. K.; Jae, R. Y. *Polym. Eng. Sci.* **1990**, *30*, 147.
- Sauceau, M.; Fages, J.; Common, A.; Nikitine, C.; Rodier, E. *Prog. Polym. Sci.* **2011**, *36*, 749.
- Arora, K. A.; Lesser, A. J.; McCarthy, T. *J. Macromolecules* **1998**, *31*, 4614.
- Baldwin, D. F.; Park, C. B.; Suh, N. P. *Polym. Eng. Sci.* **1996**, *36*, 1437.